A green approach for the preparation of ZnO@C nanocomposite using agave americana plant extract with enhanced photodegradation

Mansab Ali Jakhrani, Aneela Tahira, Muhammad Ali Bhatti, Aqeel Ahmed Shah, Nek Muhammad Shaikh, Riaz Hussain Mari, Brigitte Vigolo, Mélanie Emo, Munirah Albaqami, Ayman Nafady, et al.

A green approach for the preparation of ZnO@C nanocomposite using agave americana plant extract with enhanced photodegradation

Mansab Ali Jakhrani[1], Aneela Tahira[2], Muhammad Ali Bhatti[3], Aqeel Ahmed Shah[4], Nek Muhammad Shaikh[1], Riaz Hussain Mari[1], Brigitte Vigolo[5], Mélanie Emo[5], Munirah D. Albaqami[6], Ayman Nafady[6], Zafar Hussain Ibupoto

[1]Institute of Physics, University of Sindh Jamshoro, 76080, Sindh, Pakistan

[2]Dr. M.A Kazi Institute of Chemistry University of Sindh Jamshoro, 76080, Sindh, Pakistan

[3]Center for Environmental Sciences University of Sindh Jamshoro, 76080, Sindh, Pakistan

[4]Department of Metallurgical Engineering, NED University of Engineering and Technology, Karachi, Sindh Pakistan

[5]Université de Lorraine, CNRS, IJL, F-54000 Nancy, France

[6]Department of Chemistry, College of Science, King Saud University, Riyadh 11451, Saudi Arabia

*__Corresponding authors__: Zafar Hussain Ibupoto, **Email:** zaffar.ibhupoto@usindh.edu.pk

Abstract

The present study demonstrates the crucial role of agave americana extract in enhancing the optical properties of zinc oxide (ZnO) through thermal treatment method. Various analytical and surface science techniques have been used to identify the morphology, crystalline structure, chemical composition, and optical properties, including scanning electron microscopy (SEM), X-ray diffraction (XRD), high resolution transmission electron microscopy (HRTEM), X-ray spectroscopy (EDS) and UV-visible spectroscopy techniques. The physical studies revealed the transformation of ZnO nanorods into nanosheets upon addition of an optimized amount of agave americana extract, which induced large amount of amorphous carbon deposited onto ZnO nanostructures as confirmed by HRTEM analysis. The use of increasing amount of americana extract has significantly reduced the average crystallite size of ZnO nanostructures. The resultant hybrid system of C@ZnO has produced a significant effect on the ultraviolet light-assisted photodegradation of malachite green (MG) dye. The photocatalyst dose was fixed at 10 mg for

each study whereas the amount of agave americana extract and MG dye concentration are varied. The functionality of hybrid system was greatly enhanced when the amount of agave americana extract increased while dye concentration kept at lower level. Ultimately, almost 100% degradation efficiency was achieved via the prepared hybrid material, revealing combined contribution from synergy, stabilization of ZnO due to excess of carbon together with the high charge separation rate. The obtained results suggest that the driving role of agave americana extract for surface modification of photocatalyst can be considered for other nanostructured photocatalysts.

Keywords: Agave americana extract, ZnO nanostructures, Malachite green dye, Ultraviolet light

1. Introduction

Direct discard of industrial wastes into water makes the chronic pollution factor and consequently a big life threat to human body and environment. Pollution water is found very critical and require immediate technologies for complete removal of toxic compounds from wastewater [1-3]. A wide range of harmful substances including synthetic organic dyes are emerged the most dangerous and cause of water pollutants. The main issue is about these synthetic dyes is their high stability and limited biodegradable capability, therefore they remain in water for long time and cause sadistic effects for life. Moreover, the toxicity of synthetic dyes at minimal level in water creates a intense threat for aquatic life by blocking the passage of sunlight down to the depth of water. Among them, malachite green (MG) is known as widespread dye used in industry which impair the mammalian biological cells. MG is employed as dye for jute, paper, silk, leather products, acrylic, and wool industries. MG is also considered for the antiseptic and fungicidal products [4]. MG is effectively taken as antiprotozoal agent in various aquaculture systems [5-8]. Because of the high toxic aspects of MG and its complex molecular structure and negligible biodegradable properties, different world agencies have banned MG [9]. MG is confirmed highly and specifically carcinogenic, mutagenic and teratogenicity for both our body and aquatic animals, hence it can cause multi organ tissue destruction including breath toxicity [9-11]. These life threating aspects of MG are revealing that its complete removal from the wastewater before discharging is very crucial and requires

immediate actions. For this purpose, several techniques have been developed for the removal of MG from wastewater [12]. Many of them are based on the adsorption phenomenon and are found efficient and low cost, however the issue of secondary pollutants is emerged due to transformation of one phase of pollutant dye to another phase. Hence numerous studies have been carried out for the removal of MG from wastewater using Photodegradation technology [13-20]. The Photodegradation of MG results the nontoxic products such as CO_2, NO_2, H_2O, etc. [21-23]. The fundamental and theoretical concept of Photodegradation involve the interaction of higher energy photons than the energy band gap of photocatalyst with the surface of photocatalytic material, thereby the emergence of electron-hole pairs is observed which moves towards the surface of catalytic material [24-27]. The presence of electron donors and acceptors molecules in the reaction reacts with these electron-hole pairs, then the surface water and oxygen molecules are changed into strongly oxidizing agents like $OH/^{\cdot}O_2^-$ free radicals and consequently mineralization of dye takes place [28-30].

The nanostructured materials have been extensively investigated for the optical, chemical, and physical properties in the area wastewater treatment [30, 31]. The semiconducting metal oxides like TiO_2, ZnO, SnO_2, and WO_3 etc. have been studied intensively due to their attractive and unique features such as optical, electronic, catalytic, gas sensing, and thermal applications. Importantly, their high chemical stability is fully utilized for the purpose of wastewater treatment [32-34]. The principle of photocatalysis on the surface of semiconducting materials is based on the charge separation effectiveness of photogenerated electrons, thereby an enhancement for the photocatalysis is expected [35-37]. Among these semiconductor metal oxides, zinc oxide (ZnO) exhibits high potential for extended range of uses such as photovoltaic devices, UV laser, light emitting diodes, and gas sensing due to its high surface to volume ratio and large exciton binding energy of (60 meV) [38,39]. ZnO possesses a hexagonal wurtzite crystal array which strengthens the nucleation and anisotropic features during the growth process of nanostructured ZnO, indicating the high intensity of photogenerated electron-hole pair recombination rate at the premises of surface of ZnO [40, 41]. Another concern for ZnO is its high surface energy which enables ZnO to aggregate swiftly, therefore it is very important to tune the surface properties of not only for the dispersion in the aqueous solution but also to enhance the functionality of ZnO towards dye degradation [41]. For this purpose, chemical surface modification has been considered and used at large scale for improving the optical and stabilization properties of ZnO [39-41].

Beside this, agave americana leaves contains useful chemical compounds such as fiber (38.40%), total sugars (45.83%), and protein (35.33%), with a relatively low content in ash (5.94%) and lipid (2.03%) [42]. The main phytochemicals are structurally are enclosed in Scheme 1. Theses main phytochemicals have played a contributing role in tuning the photo activity of ZnO nanostructures and the role of phytochemicals from the agave americana leaves extract towards ZnO based photocatalysts has never been reported in the existing literature. Moreover, reported study has also shown that the agave americana leaves extract is rich with alkanes with a relative 77.7% (Maazoun, Asma Mami, et al) [43]. It is obvious that americana extract exhibits large portion of alkanes which on burning produced abundant amount of carbon in the composition of ZnO, that clearly play a significant synergetic effect role in driving the degradation of Malachite green efficiently. The agave americana plant extract is consisting the favorable chemical constituents like fibers and sugars which can play a vital role when physically mixed with ZnO nanostructures and treated at high temperature for tuning the surface properties of ZnO. Therefore, a green, low cost, simple and environmental friendly approach for the tuning the surface of properties of ZnO using agave americana plant has not been reported previously for photocatalytic applications.

In this study, we report the synthesis of ZnO nanostructures by hydrothermal method followed by the thermal treatment with agave americana extract. The use of agave americana extract changed the morphology of ZnO from crystalline nanorods to amorphous nanosheets. We have studied the morphology, crystalline quality, chemical composition by SEM, XRD and HRTEM techniques. Furthermore, thermally treated ZnO nanostructures with agave americana extract were used for the degradation of MG under the visible light. The photodegradation was studied with fixed mass of photocatalyst at varying concentrations of MG. The obtained results revealed that the agave americana extract can be useful for tuning the optical properties of other photocatalyst materials.

2. Experimental Section

2.1. Synthesis of Pure ZnO

The used chemicals were received from Sigma Aldrich, Karachi Pakistan. The pretreatment of received chemicals was not carried out. These chemicals include zinc acetate dihydrate, malachite and 25% aqueous solution of ammonia and they were of high analytical grade. Both the growth solutions of ZnO preparation and malachite degradation were prepared in the deionized water.

2.2. Preparation of agave americana extract

The leaf of agave americana plant was collected from botanical garden of University of Sindh, Jamshoro. Initially, the leaf was washed several times with deionized water to remove the dirt. Then, the small pieces of agave americana were put into the grinder machine for 30 min, then the extract was filtered and centrifuged to remove unwanted material. Finally, the collected extract was used in the precursor solution of ZnO.

2.3. Synthesis of ZnO nanostructures using hydrothermal method in the presence of agave americana extract

Hydrothermal method is low cost, environment and ecofriendly, and it offers variety for morphologies to achieve just by tailoring the hydrothermal conditions like temperature, precursors concentrations, pH of solution and use wide range of surface modifying agents. The pristine ZnO nanostructures were synthesized by hydrothermal method and used as reference for the performance evaluation of ZnO nanostructured material obtained in the presence of agave americana extract during malachite degradation. The synthesis of pristine ZnO was performed by mixing 2.22g of zinc acetate dihydrate and 5mL of (25%) aqueous ammonia solution in 100 mL of deionized water. Then mechanical stirring was done, and well dissolved precursor solution was achieved. Then beaker containing precursor's solution was sealed tightly with aluminum foil and kept at 95 ^{o}C for 5 hours in electric oven. Finally, white product of ZnO was obtained on the filter paper. Later, 0.25g of ZnO nanostructures were mixed with various amounts of agave americana extract like (2 mL, 4 mL, 6 mL and 8 mL) and thermally treated at 225 ^{o}C in air for three hours. After thermal treatment, the white ZnO turned into blackish shining due to coating carbon onto ZnO nanostructured material. The relative ratio of carbon onto ZnO was as ZnO@2mL<4mL<6m<8mL. The structural and chemical composition of pure ZnO and ZnO@ various amounts of agave americana extract were studied.

2.4. Structural characterization

The physical studies about the structure, shape, crystalline arrays, chemical composition, and functional groups were performed with wide range of analytical techniques such powder X-ray diffraction (XRD), scanning electron microscopy (SEM), high resolution transmission electron microscopy (HRTEM), Fourier transform infra-red spectroscopy (FTIR) and scanning transmission electron microscopy (STEM) coupled with energy dispersive X-ray spectroscopy (EDS). The XRD experiment was done with CuKα radiation (λ = 1.5418 Å), voltage of 45 kV, and a current of 45 mA. Scanning electron microscopy was carried out with a ZEISS Gemini SEM

500 equipped with a field emission gun. The SEM imaging was done at 3 kV. TEM and STEM micrographs were obtained using a JEOL JEM-ARM 200F apparatus equipped with a spherical aberration (Cs) probe corrector and working at an accelerating voltage of 200 kV. The powder was dispersed in ethanol, then a droplet of the dispersion was deposited on a holey carbon grid (200 mesh size). The UV-visible spectroscopy was used to monitor the photocatalytic activity of prepared nanostructured against malachite degradation under the irradiation of ultraviolet light. For the photodegradation experiment, Different aqueous solution of MG with concentrations like (8.22×10^{-5}M, 5.48×10^{-5}M and 2.74×10^{-5}M) were prepared. Then, 10mg powder of pure ZnO and ZnO@ Agave Americana extract (2mL, 4mL, 6mL and 8mL) added to each MG concentration with volume of 50mL in separate beakers. Then dye solution with photocatalyst was stirred for 30 min in the dark to reach absorption and adsorption equilibrium of dye with photocatalyst surface. Afterwards, the dye solution with photocatalyst was irradiated with ultraviolet light. The dye degradation was evaluated with 2mL aliquots from each dye concentration at regular intervals of time through the recording of absorption spectra using UV-Visible spectrophotometer of wavelength of 610 nm (PE Lamda365). The degradation efficiency of MG using ZnO nanostructures treated with different amounts of agave americana extract was calculated by degradation $\% = (A_0 - A_t)/A_0 * 100$ where A_0 is initial concentration of MG dye and A_t is the concentration of MG dye at different time intervals [44].

3. Results and discussion

3.1. Physical characterization of ZnO nanostructures prepared in the presence of agave americana extract

The diffraction patterns of various ZnO samples synthesized in the presence of different amounts of agave americana extract like (2mL, 4mL, 6mL and 8mL) are shown in Fig 1. The pure phase of ZnO diffraction pattern is included as reference phase as shown in Fig 1. The pure ZnO diffraction pattern shows all its characteristic peaks at 2θ (°) of 31.732°, 34.363°, 36.207 ° , 47.469°, 56.526°, 62.754°, 66.292°, 67.851°, 68.995°, 72.431 ° and 76.848° that corresponds to the crystal planes (100), (002), (101) , (102), (110), (103), (200), (112), (201), (004) and (202) respectively. All these measured diffraction peaks of the pure ZnO nanostructured phase correspond to the hexagonal wurtzite crystalline structure (P 6_3mc space group) with lattice parameters a = b = 3.242 Å and c = 5.188 Å according to the JCPDS card no. 01-079-0205. However, the ZnO

nanostructures prepared in the presence of agave americana extract exhibited less intense and broadened diffraction patterns, indicating the significant effect of Agave Americana extract onto the crystallographic features of ZnO as shown in Figure 1. The diffraction patterns of ZnO prepared in the presence of Agave Americana extract are well supported by the standard card (JCPD card no.01-079-0205). However, there was decrease in intensity and shift in Bragg reflections when ZnO nanostructures were thermally treated with different amounts of agave americana extract as shown in Figure 1b. This shift in the diffracted angle indicates change in the lattice parameters that may be caused by lattice micro strain that occurs as a result lattice defects, hence indicating the discolorations in ZnO crystal structure upon adding agave americana extract. There are large possibilities for the dislocation of crystallite size and consequently material is enriched by the large number of defects.

The Debye-Scherer formula was used to calculate the crystalline size of the pure ZnO and other ZnO samples prepared in the presence of agave americana extract.

$$D = K\lambda/\beta \cos\theta \qquad (1)$$

Here K is dimensionless value (i.e., 0.94), λ the X-ray wavelength (0.154060 nm), β *is* the peak intensity (FWHM) full width at half-maximum, and θ the Bragg diffraction angle [45]. The calculated average crystallite size for pure ZnO and ZnO samples prepared in the presence of agave americana extract was found 19.6 nm, 19.3 nm, 17.0 nm, 16.3 nm, and 14.6 nm respectively as given in Table1. Agave americana leaves contains useful chemical compounds such as fiber (38.40%), total sugars (45.83%), and protein (35.33%), with a relatively low content in ash (5.94%) and lipid (2.03%). The macromolecules could create a stress and defects in the crystal structure, therefore the reduction in crystallite size was expected. [46]. Morphology of pure ZnO and various ZnO samples thermally treated with different amounts of agave americana extract like (2, 4, 6 and 8 mL) was studied by SEM as shown in Figure 2. It is obvious that nanorods like morphology for the pure ZnO as shown in Figure 2a. The diameter of nanorods is found in the 150-300 nm range with an average length of several microns (Figure 2b). However, after thermal treatment of prepared ZnO nanostructures with different amounts of agave americana extract has changed the morphology of ZnO from nanorods to aggregated nanoparticles and nanosheets as shown in Figures 2c-2f. The agave americana extract contains variety chemical substance such as fiber, total sugars, and protein with a relatively low content in ash and lipid which might change the morphology of ZnO. It could be directly linked to direct use of agave americana extract for the

thermal treatment of prepared ZnO nanorods by hydrothermal method, thereby in thermal process various gases and other carbonaceous material could induce change in morphology from nanorod to nanosheets. It is also noticed that with the use of 2 mL of agave americana extract, we only see aggregated nanoparticles of ZnO with a 100-200 nm dimension as shown in Figure 2c. However, by increasing the amount from 4-8 mL of agave americana extract, nanosheets with a thickness of approximately 100 nm are shown (Figures 2d-2f).

TEM observations were carried out on the pure ZnO and the obtained micrographs are enclosed in Figure 3. Figure 3a shows that ZnO presents the same morphology of nanorods as seen by SEM (Figure 2b). The Fast Fourier Transform (FFT) obtained from HRTEM micrograph (insert of Figure 3b) shows spots which confirm the high crystalline structure of the ZnO sample. The measured inter-planar distances correspond to the hexagonal structure ($P6_3mc$, d_{001} = 0.52 nm) as already shown by the XRD study. Furthermore, TEM / STEM experiments were performed on the ZnO sample thermally treated with 8mL of agave americana extract. As obtained by SEM, the nanosheet-like morphology of particles was observed by TEM (Figure 4a). Contrarily to the pure ZnO sample, the FFT obtained from HRTEM micrograph revealed that ZnO sample with agave americana extract is a mixture of amorphous and polycrystalline phases (insert Figure 4b). The measured interplanar distances of polycrystalline structure correspond to the hexagonal structure of ZnO ($P6_3mc$, d_{100} = 0.28 nm). Complementary X-mapping was done, and the particles are uniformly composed of Zn, O and C (Figures 4c-f).

The FTIR measurement was used to identify the functional groups and the Zn-O chemical bonding as shown in Figure 5. Typical Z-O stretching vibration was noticed 529 cm^{-1}. The characteristic bands around 1026 cm^{-1} and 1429 cm^{-1} was indexed to C-O and C-N stretching bands. The surface bound hydroxyl band is assigned at 3437 cm^{-1} as shown in Figure 5a. All the observed bands of ZnO are well matching to the published work [47]. For the malachite, the bands in the range of 500 -1500 cm^{-1} were linked to mono and para-di substituted benzene ring. At the same time band features from 50 0 - 700 $cm^{-1}$are attributed to sulfide and bromine groups in the benzene ring of malachite as shown in Figure 5b. The band around 1112 cm^{-1} suggests the C-N stretching and asymmetric band of methyl group was found at 2925 cm^{-1}revealing the typical features of pure malachite green as described in already published work [48]. For the use of agave americana plant extract with ZnO, it has altered the band position of ZnO as shown in Fig. 5c. At the complete degradation of MG, the most of bands of MG were disappeared on the surface of ZnO, confirming

the potential effectiveness of agave americana plant extract for tuning the optical properties of ZnO during photocatalysis [48].

3.2. Photodegradation of MG dye using thermally treated ZnO nanostructured material

The MG was dissolved into the deionized water and before the degradation reaction and mechanical stirring of MG with photocatalyst was performed in order to achieve physical adsorption and absorption equilibrium for 30 min. However, we did not evaluate the adsorption but we have observed that the adsorption of dye before degradation reaction could be around 5-6%. Afterwards, the photocatalysis was carried out that has selectively removed the dye from the aqueous solution and mineralized MG dye into water. The photodegradation of MG was evaluated with fixed photocatalyst dose of 10 mg of various ZnO samples including pristine and thermally treated with different amounts of agave americana extract. Afterwards, the photodegradation phenomenon was studied by recording UV-visible light absorption spectra for the 8.22×10^{-5}M of MG and the degradation rate was monitored for the time interval of 25-200 min using ultraviolet light. The photocatalytic activity of pure ZnO against MG is shown in Figure 6a and a slight decrease in the absorption is confirming the poor performance from pure ZnO as expected. At the same time, we have studied the kinetics of MG degradation under natural sunlight using pure ZnO and the kinetics is followed by the 1^{st} and 2^{nd} order pseudo kinetics as shown in Figure 6 (b,c). The MG removal efficiency was noticed for pure ZnO in the order at different time intervals like (51.2%, 54.0%, 57.8%, 61.1%, 63.4%, 65.4%, 67.8% and 70.1%) and 25, 50, 75, 100, 125, 150, 175 and 200 min respectively as shown in Figure 6d. The poor performance of pure ZnO towards MG degradation under the ultraviolet light could be assigned to high recombination rate of electron and holes, thereby a minimum number of catalytic sites further limit the performance of pure ZnO towards MG degradation [49]. For studying our targeted ZnO material thermally treated with various amounts of agave americana extract (2 mL, 4mL, 6mL, and 8mL), similar MG 8.22×10^{-5}M of MG and 10 mg photocatalyst dose were used. It was found that degradation rate became faster for the time intervals of (20, 40, 60, 80, 100, 120 and 140 min) respectively, as shown in Fig. 7a-d. Interestingly, the degradation became prominent when the ZnO sample was thermally treated with higher amount of agave americana extract like 8mL. The presence of more carbon content into ZnO sample, has drastically lifted the photodegradation process due to more quantity of active sites, defects in the structure, and low charge recombination rate of electron and holes, revealing more radical's generation during the irradiation of light thereby swift oxidation of MG

is demonstrated [32, 36, 37, 38]. The relative degradation efficiency for the ZnO samples thermally treated with 2 mL, 4 mL, 6 mL, and 8 mL of agave americana extract was in order of 90.7%, 94.5%, 95.4% and 97.5% for the time intervals of 20-140 min respectively (Fig.8a-d). From these observations, it is clear that increasing the quantity of agave americana extract is enhancing the degradation process kinetics due to increasing amount of carbon [43], which synergistically with ZnO increased the degradation process efficiently. The increased degradation efficiency is confirming that agave americana extract has potentially enhanced the photocatalytic features of ZnO towards MG dye degradation. Therefore, agave americana extract can be a great opportunity for the tuning the functional properties of other photocatalytic materials. The kinetics studies of MG degradation with the use of ZnO samples treated with agave americana extract followed 1st and 2nd pseudo-order kinetics.

3.3. Effect of initial dye concentration

The role of different amounts of agave americana extract for enhancing the photocatalytic activity of ZnO was studied for higher concentrations of MG dye such as 8.22×10^{-5}M, 5.48×10^{-5}M and 2.74×10^{-5}M. At low concentration 5.48×10^{-5}M of MG dye, the degradation rate was highly significant, indicating that dye concentration during the photocatalysis of ZnO thermally treated with agave americana extract is very critical. The use of fixed 10 mg of ZnO samples thermally treated with 2, 4, 6 and 8 mL of agave americana extract has shown dramatic decrease in absorption spectra for time interval of 15-90 min as shown in Figure (9a-d). The degradation efficiency of MG dye for (5.48×10^{-5}M) concentration using ZnO samples thermally treated with various amounts of 2, 4, 6 and 8 mL of agave americana extract were found as 85.2%, 90.2%, 91.8%, 92.8%, 93.65% and 94.0%, for 4mL;85.9%, 90.6%, 91.8%, 92.8%, 94.3% and 94.9% for 6mL; 86.1%, 90.8, 91.9%, 93.1%, 94.7% and 96.0 whereas, for 8mL; 86.9%, 91.0%, 93.2%, 94.8%, 96.15 and 97.5% respectively for the time interval of 15-90 min as shown in Fig10c. Furthermore, the photocatalytic activity of ZnO nanostructures thermally treated with various amounts of agave americana extract was investigated in low concentration of 2.74×10^{-5} MG dye as shown in Figure 11a-d. It was observed that the degradation rate became very fast and MG dye almost 100% degraded in a time interval of 10-60 min. These results confirms that agave americana extract with plenty of phytochemicals see Scheme 1, and high amount of alkaline compounds [43], they together effectively improved the photocatalytic properties of ZnO towards the degradation of MG

under the irradiation of UV light. Again, the superfast MG dye degradation was found with the ZnO sample treated with highest amount of 8 mL of agave americana extract. The degradation kinetics was studied via Langmuir-Hinshewood equation as shown in Fig 12a and the straight line reveals that the degradation kinetics of MG was followed by 1st order kinetics and calculated rate constants values for various samples of ZnO for dye concentration of 2.74×10^{-5}M, 5.48×10^{-5}M, and 8.22×10^{-5}M are enclosed in Table 2. It is obvious from the Table 2, that the value of rate constant is highest for the ZnO sample thermally treated with 8mL of agave americana extract for all dye concentrations, evidently in the lowest concentration of MG dye, the rate constant is significantly high. From the reaction kinetics study, it is obvious that the higher amount of agave americana extract has potentially tuned the surface catalyst sites of ZnO and modified the surface for favorable MG dye degradation rate. This confirms the dye concentration dependent performance of as prepared ZnO based photocatalys irrespective of same photocatalyst dose of material for both the pristine ZnO and agave americana extract assisted ZnO nanostructured photocatalyst . The dye degradation is faster as expected at low concentration since light photons easily interact with the surface of photocatalyst, thereby large number of oxidizing radicals could be observed, hence efficient degradation process was demonstrated. However, at high concentration of MG dye, the photons of light face a large barrier in interacting with the surface of photocatalyst, hence a limited number of oxidizing radicals are produced, therefore photodegradation reaction kinetics is less likely poor [50]. A proposed MG dye degradation mechanism is represented by Figure 13. The possible generation of reaction steps are described below:

$MG^{*}{}_{ads} + ZnO \longrightarrow MG^{\bullet+} + ZnO_{(e-)}$

$ZnO_{(e-)} + O_2 \longrightarrow O^{\bullet-}{}_2$

$ZnO_{(h+)} + OH^- \longrightarrow OH^{\bullet}$

$OH^{\bullet}$ or $O^{\bullet-}{}_2 + MG^{\bullet+} \longrightarrow$ degraded products

$OH^{\bullet}$ or $O_2^{\bullet-} + MG_{ads} \longrightarrow$ degraded products

When the light photons interact with the surface of green MG dye, then many of them are absorbed it and consequently electrons are produced which are moved towards the conduction band of ZnO nanostructures. Afterwards, the excited electrons are reacting with the dissolved oxygen and water molecules, then it results the formation of superoxide radicals ($O_2^{\bullet-}$). At the same time, the hydroxyl radicals are produced due to the reactive nature of superoxide ions with the surface bound water molecules. The malachite dye being cationic in nature through the interaction with

superoxide and hydroxyl radicals started to degrade via radical mechanism [51]. Importantly, it has been identified by previous studies that the degradation of MG dye is mainly occurring due to the superoxide ions and consequently a harmful dye is changed into harmless products.

Generally, the selective photodegradation of cationic dyes from wastewater are connected to the electrostatic interaction between the cationic dye and negative surface of photocatalyst and it is well supported by the reported works [52, 53]. Furthermore, the selectivity of MG dye is describe by its cationic nature owing its favorable chemical structure of MG which strongly bound to the negative surface of n-type ZnO semiconducting material [54].

The photocatalytic assessment was studied by considering the achieved results with low dye concentration of MG as given in Table 3 [55-68]. And the obtained results are equal or superior to the reported works in terms of performance, low-cost fabrication, simple and green nature of material synthesis approach. From Table 3, it is obvious that proposed strategy of designing the nanocomposite is associated with the use of minimum toxic chemicals, environment and ecofriendly, and these features enable it to be highly desirable for large scale production of material. The surface modification of ZnO by sugars and fibrous materials from agave americana extract, led to enhance the photodegradation efficiency of approximately 100% as clearly can be seen from Table 3. The superior performance of as prepared C@ZnO nanocomposite could be assigned to crystal defects, high carbon content, reduction in average crystallite size, and high density of active sites. In the published work [67], authors have used the plant extract and combusted at different temperatures which further impose the high cost of electricity consumption for the design of photocatalyst. We understand the reaction time is short compare to our study, as they have used same MG concentration to that of us but with high photocatalyst dose. It is true that by increasing the photocatalyst dose, the performance of dye degradation can be enhanced. Keeping in view the low photocatalyst dose and low cost production of ZnO in our work has superior advantages to capitalize for the practical applications compare to the previous work [67]. However, the performance of our material is equal to that of published work [67]. In the published work [68], the two materials like ZnO and TiO_2 were prepared and studied for the degradation of MG, however the synthesis process is relatively expensive and complicated as it involve several chemicals and steps which can produce the toxicity during the synthesis process. However, in our work we have only used ZnO with americana extract which decrease the cost of material synthesis, avoids the use of many chemicals, high probability of environment friendly nature and offers large

scale production of material from the earth abundant sources like americana extract. These are advantageous features of our work for the degradation of MG with superior or equal degradation efficiency compare to the previous published works.

4. Conclusions

In this contribution, we studied the effect of agave americana extract with various amounts to the thermally treated ZnO nanostructures prepared by hydrothermal. The prepared hybrid C@ZnO system consists of an amorphous feature due to rich amount of carbon material and it has proven to be an efficient photocatalyst for the removal of malachite green (MG) under ultraviolet light. Owing to the large number of sugars and fibers found in the agave americana extract, its addition to the crystal structure of ZnO results in dramatic change in crystal structure and creates lattice defects. And they have played a dynamic role on tuning the optical properties of ZnO and enhancing the charge separation rate of electron/holes, consequently an outperform functionality is demonstrated. Evidently, this method of using agave americana extract under thermal treatment for the modification of any prepared photocatalyst material may pave the way for the low cost wastewater treatment.

Acknowledgments

We would like to thank the platform “Microscopies, Microprobes and Metallography (3M)” (Institut Jean Lamour, IJL, Nancy, France) for TEM and SEM facilities and J. Ghanbaja for his valuable help for TEM analyses. We also extend sincere appreciation for the Researchers Supporting Project (RSP-2022/79) at King Saud University, Riyadh, Saudi Arabia for partial support of this work.

Conflict of Interest

Authors declare no conflict of interest in this study

5. References

[1]. Pollard SJT. Fowler GD, Sollars CJ and Perry R 1992 Low-cost adsorbents for waste and wastewater treatment: a review. *Science of the total environment*. ***116***(1-2) 31-52.

[2]. Gupta VK, Ali I, Saleh TA, Nayak A and Agarwal S 2012 Chemical treatment technologies for waste-water recycling—an overview. *Rsc Advances*. ***2*** 6380-6388.

[3]. Sagir M and Tahir MB 2021 Role of Nanocatalyst (Photocatalysts) for Waste Water Treatment. *Current Analytical Chemistry*. ***17*** 138-149.

[4]. Raval NP, Shah PU and Shah NK 2017 Malachite green "a cationic dye" and its removal from aqueous solution by adsorption. *Applied Water Science*, *7*(7), pp.3407-3445.

[5]. Yong L, Zhanqi G, Yuefei J, Xiaobin H, Cheng S, Shaogui Y, Lianhong W, Qingeng W and Die F 2015 Photodegradation of malachite green under simulated and natural irradiation: kinetics, products, and pathways. *Journal of Hazardous Materials.* ***285*** 127-136.

[6]. El-Hout SI, El-Sheikh, SM, Gaber A, Shawky A and Ahmed AI 2020 Highly efficient sunlight-driven photocatalytic degradation of malachite green dye over reduced graphene oxide-supported CuS nanoparticles. *Journal of Alloys and Compounds*. ***849*** 156573.

[7]. Verma M, Mitan M, Kim H and Vaya D 2021 Efficient photocatalytic degradation of Malachite green dye using facilely synthesized cobalt oxide nanomaterials using citric acid and oleic acid. *Journal of Physics and Chemistry of Solids*. ***155*** 110125.

[8]. Munyai S, Tetana ZN, Mathipa MM, Ntsendwana B and Hintsho-Mbita NC 2021 Green synthesis of Cadmium Sulphide nanoparticles for the photodegradation of Malachite green dye, Sulfisoxazole and removal of bacteria. *Optik*. ***247*** 167851.

[9]. Panahian Y and Arsalani N 2017 Synthesis of hedgehoglike F-TiO2 (B)/CNT nanocomposites for sonophotocatalytic and photocatalytic degradation of malachite green (MG) under visible light: kinetic study. *The Journal of Physical Chemistry A*. ***121*** 5614-5624.

[10]. Ismail NJ, Zakria HS, Noor SM, Othman MHD, Rahman MA, Jaafar J and Ismail AF 2021 Photocatalytic Nanocomposites for Environmental Remediation. In *Functional Hybrid Nanomaterials for Environmental Remediation.* 161-186.

[11]. Jassal V, Shanker U, Kaith BS and Shankar S 2015 Green synthesis of potassium zinc hexacyanoferrate nanocubes and their potential application in photocatalytic degradation of organic dyes. *RSC Advances*. ***5*** 26141-26149.

[12]. Tewari K, Singhal G and Arya RK 2018 Adsorption removal of malachite green dye from aqueous solution. *Reviews in Chemical Engineering*. ***34*** 427-453.

[13]. Qasim S, Zafar A, Saif MS, Ali Z, Nazar, M, Waqas M, Haq AU, Tariq T, Hassan SG, Iqbal F and Shu XG 2020 Green synthesis of iron oxide nanorods using Withania coagulans extract improved photocatalytic degradation and antimicrobial activity. *Journal of Photochemistry and Photobiology B: Biology*. ***204*** 111784.

[14]. Heidarpour H, Golizadeh M, Padervand M, Karimi A, Vossoughi M and Tavakoli MH 2020 In-situ formation and entrapment of Ag/AgCl photocatalyst inside cross-linked carboxymethyl cellulose beads: A novel photoactive hydrogel for visible-light-induced photocatalysis. *Journal of Photochemistry and Photobiology A: Chemistry*. ***398*** 112559.

[15]. ernández-Oloño JT, Infantes-Molina A, Vargas-Hernández D, Domínguez-Talamantes DG, Rodríguez-Castellón E, Herrera-Urbina JR and Tánori-Córdova, JC 2021 A novel heterogeneous photo-Fenton Fe/Al2O3 catalyst for dye degradation. *Journal of Photochemistry and Photobiology A: Chemistry*. ***421*** 113529.

[16]. Almutairi FM, El Rabey HA, Alalawy AI, Salama AA, Tayel, AA, Mohammed GM, Aljohani MM, Keshk AA, Abbas NH and Zayed MM 2021. Application of Chitosan/Alginate Nanocomposite Incorporated with Phycosynthesized Iron Nanoparticles for Efficient Remediation of Chromium. *Polymers*. ***13*** 2481.

[17]. Ortiz-Zarco E, Solis-Casados D, Escobar-Alarcón L and García-Orozco I 2022 Visible light-driven photocatalyst: An iron (III) coordination compound in Rhodamine B degradation. *Journal of Photochemistry and Photobiology A: Chemistry*. ***424*** 113629.

[18]. Seraghni N, Dekkiche BA, Debbache N, Belattar S, Mameri Y, Belaidi S and Sehili T 2021 Photodegradation of cresol red by a non-iron Fenton process under UV and sunlight irradiation: Effect of the copper (II)-organic acid complex activated by H2O2. *Journal of Photochemistry and Photobiology A: Chemistry* ***420*** 113485.

[19]. Lerici LC, Marchena CL, Torres CC, Campos CH and Pierella LB 2022 Fe-doped Al2O3 nanoplatforms as efficient and recyclable photocatalyst for the dyes remediation. *Journal of Photochemistry and Photobiology A: Chemistry*. ***426*** 113733.

[20]. Karadeniz D, Kahya N and Erim FB 2022 Effective photocatalytic degradation of malachite green dye by Fe (III)-Cross-linked Alginate-Carboxymethyl cellulose composites. *Journal of Photochemistry and Photobiology A: Chemistry*. ***428*** 113867.

[21]. Zhang C, Li N, Chen D, Xu Q, Li H, He J and Lu J 2021 The ultrasonic-induced-piezoelectric enhanced photocatalytic performance of ZnO/CdS nanofibers for degradation of bisphenol A. *Journal of Alloys and Compounds*. ***88*** 160987.

[22]. Hosseini A, Foroughi J, Sabzehmeidani MM and Ghaedi M 2021 Heterogeneous photoelectro-Fenton using ZnO and TiO2 thin film as photocatalyst for photocatalytic degradation Malachite Green. *Applied Surface Science Advances*. ***6*** 100126

[23]. Sui G, Li J, Du L, Zhuang Y, Zhang Y, Zou Y and Li B 2020 Preparation and characterization of g-C3N4/Ag–TiO2 ternary hollowsphere nanoheterojunction catalyst with high visible light photocatalytic performance. *Journal of Alloys and Compounds*. ***823*** 153851.

[24]. Kumar S, Kaushik RD and Purohit LP 2022 ZnO-CdO nanocomposites incorporated with graphene oxide nanosheets for efficient photocatalytic degradation of bisphenol A, thymol blue and ciprofloxacin. *Journal of Hazardous Materials*. ***424*** 127332.

[25]. Ahmadi S and Ganjidoust H 2021 Using banana peel waste to synthesize BPAC/ZnO nanocomposite for photocatalytic degradation of Acid Blue 25: Influential parameters, mineralization, biodegradability studies. *Journal of Environmental Chemical Engineering*. ***9*** 106010.

[26]. Jia S, Li J, Sui G, Du L, Zhang Y, Zhuang Y and Li B 2019 Synthesis of 3D flower-like structured Gd/TiO 2@ rGO nanocomposites via a hydrothermal method with enhanced visible-light photocatalytic activity. *RSC advances*. ***9*** 31177-31185.

[27]. Poce-Fatou, J.A., Gil, M.L.A., Alcantara, R., Botella, C. and Martin, J., 2004. A photochemical reactor for the study of kinetics and adsorption phenomena. *Journal of chemical education*, *81*(4), p.537.

[28]. Li J, Li B, Sui G, Du L, Zhuang Y, Zhang Y and Zou Y 2021 Removal of volatile organic compounds from air using supported ionic liquid membrane containing ultraviolet-visible light-driven Nd-TiO2 nanoparticles. *Journal of Molecular Structure*. ***1231*** 130023.

[29]. Avciata O, Benli Y, Gorduk S and Koyun O 2016 Ag doped TiO2 nanoparticles prepared by hydrothermal method and coating of the nanoparticles on the ceramic pellets for photocatalytic study: Surface properties and photoactivity. *Journal of Engineering Technology and Applied Sciences*. ***1*** 34-50.

[30]. Wu S, Lin Y and Hu YH 2021 Strategies of tuning catalysts for efficient photodegradation of antibiotics in water environments: A review. *Journal of Materials Chemistry A*. ***9*** 2592-2611.

[31]. Mondal K 2017 Recent advances in the synthesis of metal oxide nanofibers and their environmental remediation applications. *Inventions*. ***2*** 9.

[32]. Cardoso IM, Cardoso RM and da Silva JC 2021 Advanced Oxidation Processes Coupled with Nanomaterials for Water Treatment. *Nanomaterials*. ***11*** 2045.

[33]. Ahmad NA, Goh PS, Zulhairun AK, Wong TW and Ismail AF 2021 The Role of Functional Nanomaterials for Wastewater Remediation.

[34]. Gautam RK and Chattopadhyaya MC 2016 Chapter 13-Nanomaterials in the Environment: Sources, Fate, Transport, and Ecotoxicology. *Nanomaterials for Wastewater Remediation; Gautam, RK, Chattopadhyaya, MC, Eds*. 311-326.,

[35]. Anjum M, Miandad R, Waqas M, Gehany F and Barakat MA 2019 Remediation of wastewater using various nano-materials. Arab J Chem. **12** 4897–4919.

[36]. Vasantharaj S, Sathiyavimal S, Senthilkumar P, Kalpana VN, Rajalakshmi G, Alsehli M, Elfasakhany A and Pugazhendhi A 2021 Pugazhendhi, Enhanced photocatalytic degradation of water pollutants using bio-green synthesis of zinc oxide nanoparticles (ZnO NPs), J. Environ. Chem. Eng. **9** 105772

[37]. Anitha J, Selvakumar R, Hema S, Murugan K and Premkumar T 2022 Facile green synthesis of nano-sized ZnO using leaf extract of Morinda tinctoria: MCF-7 cell cycle arrest, antiproliferation, and apoptosis studies. *Journal of Industrial and Engineering Chemistry*. ***105*** 520-529.

[38]. Chan YY, Pang YL, Lim S and Chong WC 2021 Facile green synthesis of ZnO nanoparticles using natural-based materials: Properties, mechanism, surface modification and application. *Journal of Environmental Chemical Engineering*. ***9*** 105417.

[39]. Balasubramanian R, Srinivasan R and Lee J 2021 Barrier, rheological, and antimicrobial properties of sustainable nanocomposites based on gellan gum/polyacrylamide/zinc oxide. *Polymer Engineering & Science*, *61*(10), pp.2477-2486.
[40]. Wang Z, Bockstaller MR and Matyjaszewski K 2021 Synthesis and applications of ZnO/polymer nanohybrids. *ACS Materials Letters*. ***3*** 599-621.
[41]. Divya M, Vaseeharan B, Abinaya M, Vijayakumar S, Govindarajan M, Alharbi NS, Kadaikunnan S, Khaled JM and Benelli G 2018 Biopolymer gelatin-coated zinc oxide nanoparticles showed high antibacterial, antibiofilm and anti-angiogenic activity. *Journal of Photochemistry and Photobiology B: Biology*. ***178*** 211-218.
[42]. Bouaziz MA, Rassaoui R and Besbes S 2014 Chemical composition, functional properties, and effect of inulin from tunisian Agave americana L. Leaves on textural qualities of pectin gel. *Journal of Chemistry*. *2014*.
[43]. Maazoun AM, Hamdi SH, Belhadj F, Jemâa JM, Messaoud C and Marzouki MN 2019 Phytochemical profile and insecticidal activity of Agave americana leaf extract towards Sitophilus oryzae (L.)(Coleoptera: Curculionidae). Environmental Science and Pollution Research. **19** 19468-80.
[44]. Aminuzzaman M, Ying LP, Goh WS and Watanabe A 2018 Green synthesis of zinc oxide nanoparticles using aqueous extract of Garcinia mangostana fruit pericarp and their photocatalytic activity. *Bulletin of Materials Science*. ***41*** 1-10.
[45]. Zhang X, Chen Y, Zhang S and Qiu C 2017 High photocatalytic performance of high concentration Al-doped ZnO nanoparticles. *Separation and Purification Technology*. ***172*** 236-241.
[46]. Küünal S, Rauwel P and Rauwel E 2018 Plant extract mediated synthesis of nanoparticles. In *Emerging applications of nanoparticles and architecture nanostructures*. 411-446. Elsevier.
[47]. Saad AHA, Azzam AM, El-Wakeel ST, Mostafa BB and Abd El-latif MB 2018 Removal of toxic metal ions from wastewater using ZnO@ Chitosan core-shell nanocomposite. *Environmental Nanotechnology, Monitoring & Management*. ***9*** 67-75.
[48]. Saravanakumar K and Kathiresan K 2014 Bioremoval of the synthetic dye malachite green by marine Trichoderma sp. *SpringerPlus*. ***3*** 1-12.
[49]. Soto-Robles CA, Luque PA, Gómez-Gutiérrez CM, Nava O, Vilchis-Nestor AR, Lugo-Medina E, Ranjithkumar R and Castro-Beltrán A 2019 Study on the effect of the concentration of Hibiscus sabdariffa extract on the green synthesis of ZnO nanoparticles. *Results in Physics*. ***15*** 102807.
[50]. Davis RJ. Neal GO and Wenwu I 1994 *Water Environ. Res.* **66** 50.
[51]. Huang ST, Jiang YR, Chou SY, Dai YM and Chen CC 2014 Synthesis, characterization, photocatalytic activity of visible-light-responsive photocatalysts BiOxCly/BiOmBrn by controlled hydrothermal method. *Journal of Molecular Catalysis A: Chemical*. ***391*** 105-120.
[52]. Araya T, Chen C, Jia M, Johnson D, Li R, Huang Y 2017 Selective degradation of organic dyes by a resin modified Fe-based metal-organic framework under visible light irradiation**.** Optical Materials. ***64*** 512-523

[53]. Ekmen E, Bilici M, Turan E, Tamer U, Zengin A 2020 Surface molecularly-imprinted magnetic nanoparticles coupled with SERS sensing platform for selective detection of malachite green.Sensors. Actuators B. ***325*** 128787

[54]. Anupama RP, Julia G, Shamsheera KO, lAbraham J 2019 Bio-inspired green synthesis of zinc oxide nanoparticles using Abelmoschus esculentus mucilage and selective degradation of cationic dye pollutants, Journal of Physics and Chemistry of Solids. ***127*** 265-274

[55]. Sharma G, ALOthman ZA, Kumar A, Sharma S, Ponnusamy SK and Naushad M 2017 Fabrication and characterization of a nanocomposite hydrogel for combined photocatalytic degradation of a mixture of malachite green and fast green dye. *Nanotechnology for Environmental Engineering*. ***2*** 1-7.

[56]. Meena S, Vaya D and Das BK 2016 Photocatalytic degradation of Malachite Green dye by modified ZnO nanomaterial. *Bulletin of Materials Science*. ***39*** 1735-1743.

[57]. Amar IA, Harara HM, Baqul QA, Abdul Qadir MA, Altohami FA, Ahwidi MM, Abdalsamed IA and Saleh FA 2020 Photocatalytic degradation of malachite green dye under UV light irradiation using calcium-doped ceria nanoparticles. *Asian Journal of Nanosciences and Materials*. ***3*** 1-14..

[58]. El-Hout SI, El-Sheikh SM, Gaber A, Shawky A and Ahmed AI 2020 Highly efficient sunlight-driven photocatalytic degradation of malachite green dye over reduced graphene oxide-supported CuS nanoparticles. *Journal of Alloys and Compounds*. ***849*** 156573.

[59]. Aminuzzaman M, Ying LP, Goh WS and Watanabe A 2018 Green synthesis of zinc oxide nanoparticles using aqueous extract of Garcinia mangostana fruit pericarp and their photocatalytic activity. *Bulletin of Materials Science*. ***41*** 1-10.

[60]. Ameta KL, Papnai N and Ameta R 2014 Photocatalytic degradation of Malachite Green using nano-sized cerium-iron oxide. *Orbital: The Electronic Journal of Chemistry*. ***6*** 14-19

[61]. Malik JH, Zaman MB, Poolla R, Malik KA, Assadullah I, Bhat AA and Tomar R 2021. Hydrothermal synthesis of tetragonal and wurtzite Cu2MnSnS4 nanostructures for multiple applications: Influence of different sulfur reactants on growth and properties. *Materials Science in Semiconductor Processing*. ***121*** 105438.

[62]. Mark JA, Venkatachalam A, Pramothkumar A, Senthilkumar N, Jothivenkatachalam K and prince Jesuraj J 2021. Investigation on structural, optical and photocatalytic activity of CoMn2O4 nanoparticles prepared via simple co-precipitation method. *Physica B: Condensed Matter*. ***601*** 412349.

[63]. Yulizar Y, Eprasatya A, Apriandanu DO and Yunarti RT 2021 Facile synthesis of ZnO/GdCoO3 nanocomposites, characterization and their photocatalytic activity under visible light illumination. *Vacuum*. ***183*** 109821.

[64]. Bhatti MA, Tahira A, Almani KF, Bhatti AL, Waryani B, Nafady A and Ibupoto ZH 2021. Enzymes and phytochemicals from neem extract robustly tuned the photocatalytic activity of ZnO for the degradation of malachite green (MG) in aqueous media. *Research on Chemical Intermediates*. ***47*** 1581-1599.

[65]. Huang Q, Chen C, Zhao X, Bu X, Liao X, Fan H, Gao W, Hu H, Zhang Y and Huang Z 2021. Malachite green degradation by persulfate activation with CuFe2O4@ biochar composite: Efficiency, stability and mechanism. *Journal of Environmental Chemical Engineering*. ***9*** 105800.

[66]. Verma M, Mitan M, Kim H and Vaya D 2021 Efficient photocatalytic degradation of Malachite green dye using facilely synthesized cobalt oxide nanomaterials using citric acid and oleic acid. *Journal of Physics and Chemistry of Solids*. ***155*** 110125.

[67]. Sukri SN, Isa ED and Shameli K 2020 Photocatalytic degradation of malachite green dye by plant-mediated biosynthesized zinc oxide nanoparticles. InIOP Conference Series: Materials Science and Engineering. **808** 012034.

[68]. Hosseini A, Foroughi J, Sabzehmeidani MM 2021 Ghaedi M. Heterogeneous photoelectro-Fenton using ZnO and TiO2 thin film as photocatalyst for photocatalytic degradation Malachite Green. Applied Surface Science Advances. **6** 100126.

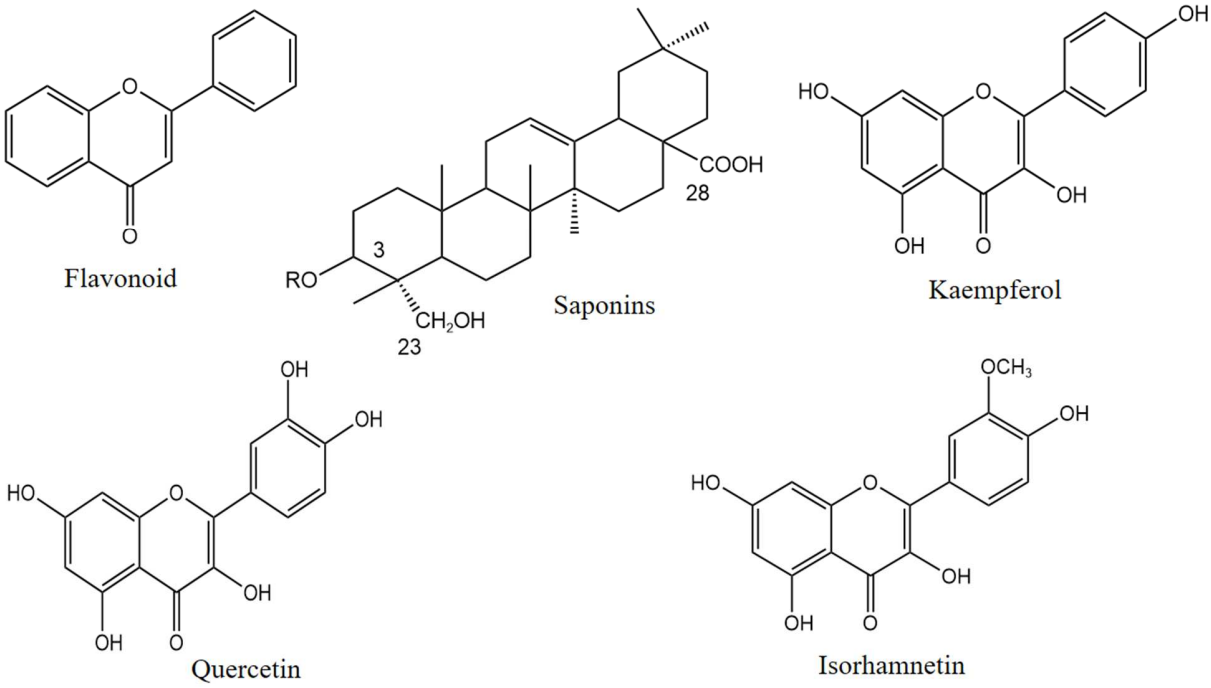

Scheme 1. Phytochemical profile of agave americana extract

Figure captions

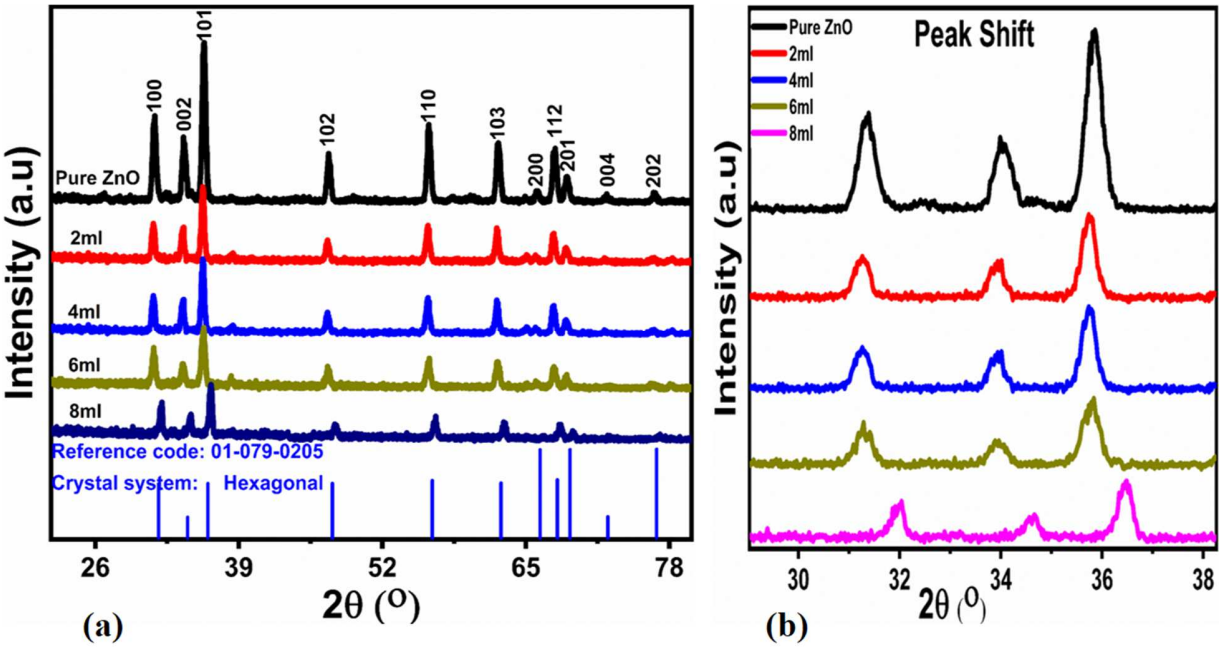

Figure 1. (a) Powder XRD patterns of pure ZnO prepared with various concentrations of agave americana extract **(b)** illustrate the shift in (100), (002) and (101) Bragg reflections with agave americana leaves concentration

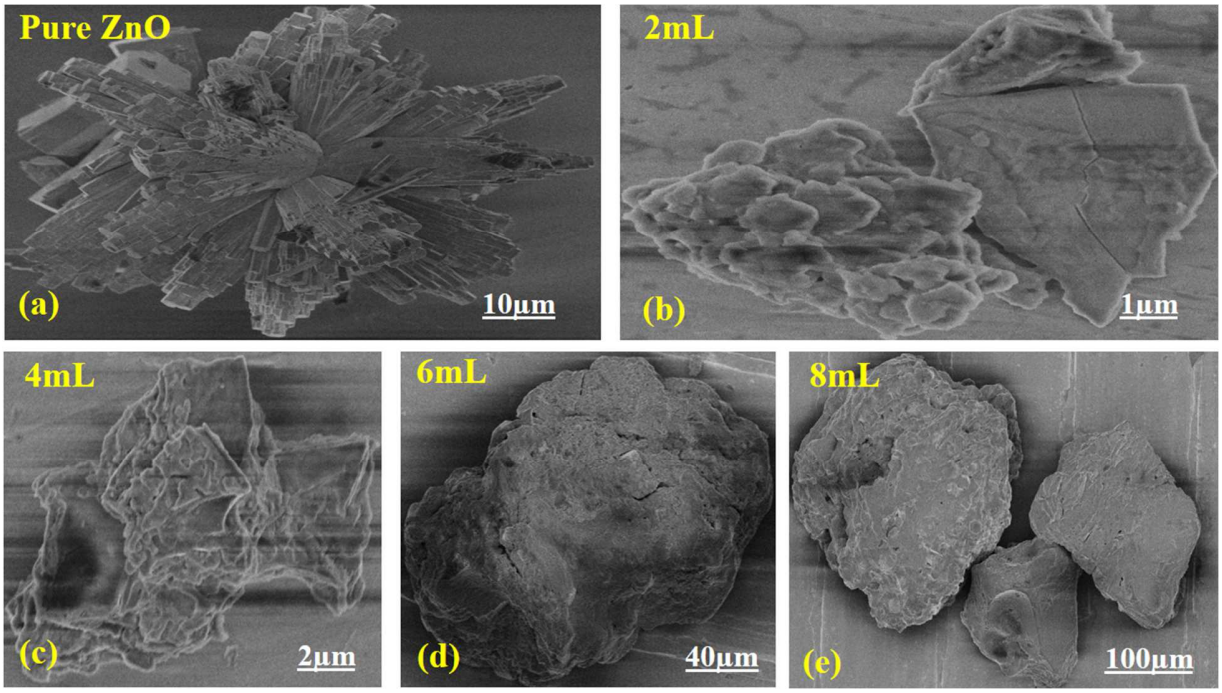

Figure 2: SEM images of **(a)** pure ZnO, **(b-d)** ZnO nanostructures thermally treated with different amounts of agave americana extract (2, 4, 6 and 8 mL).

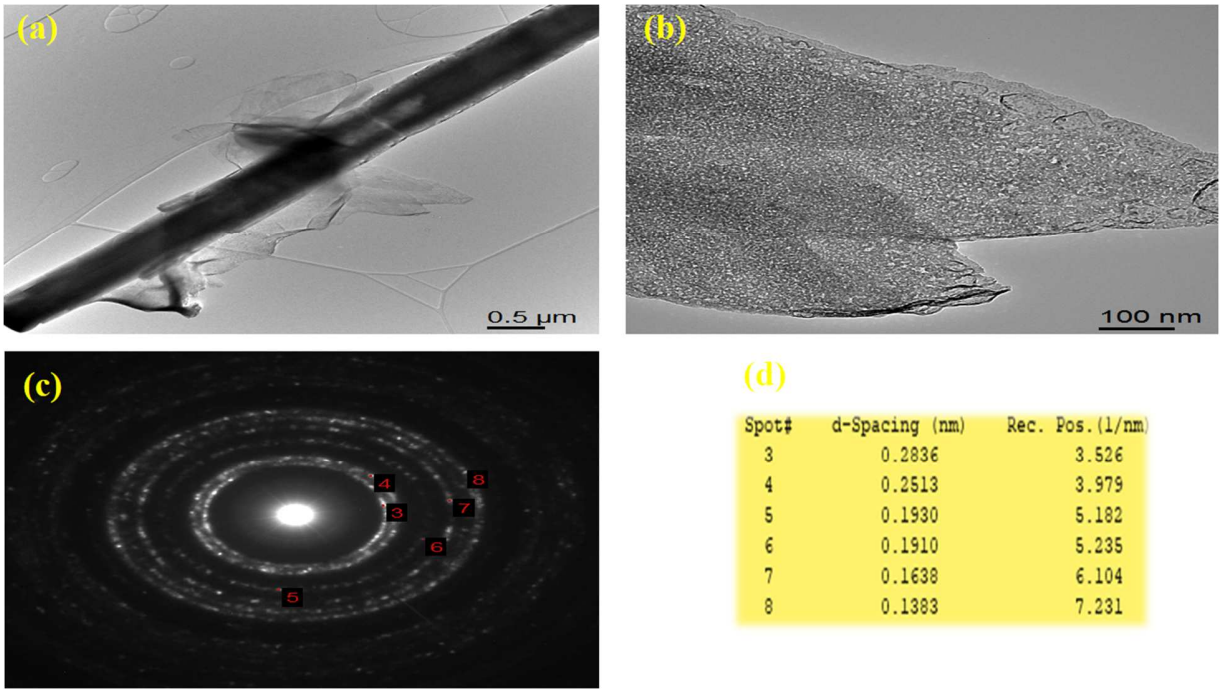

Figure 3: TEM-HRTEM and SAED images of pure ZnO prepared by hydrothermal method

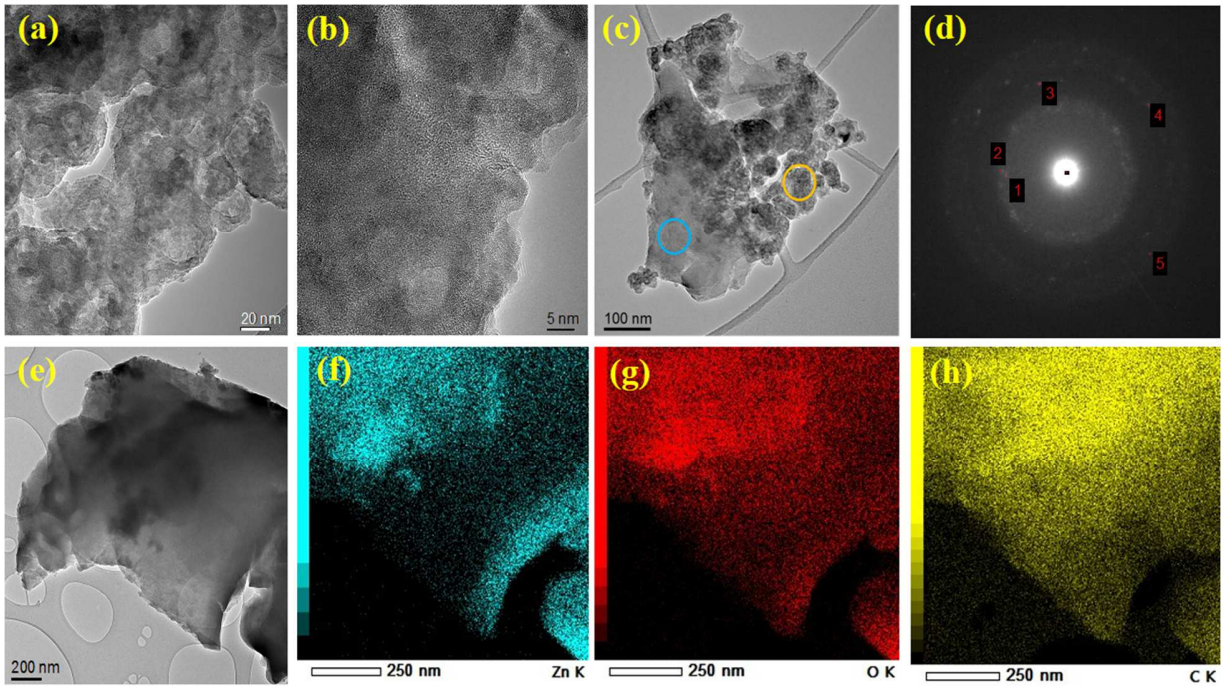

Figure 4: **(a-c)** HRTEM images of ZnO sample thermally treated with 8 mL of agave americana extract, **(d)** SAED patterns, **(e)** TEM image, **(f-h)** Elemental mapping

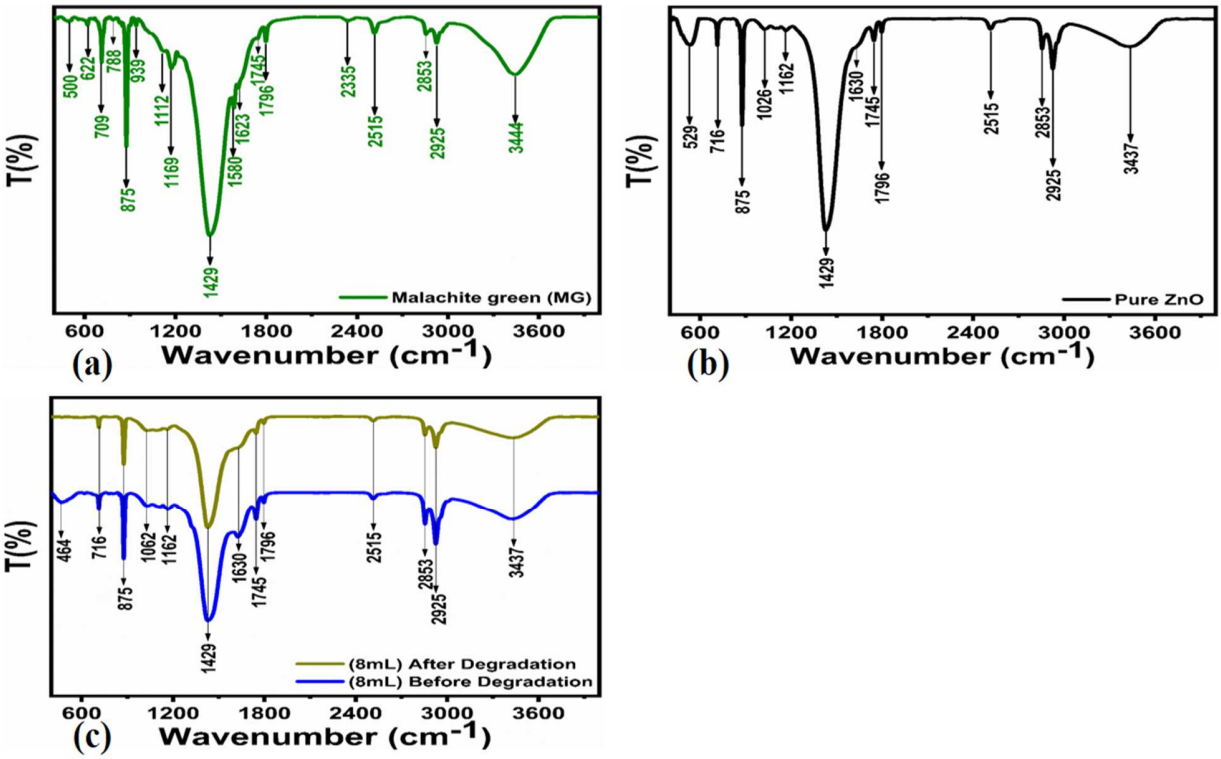

Figure 5. **(a)** FTIR spectra of MG, **(b)** FTIR spectra of pure ZnO **(c)** FTIR spectra of ZnO prepared in the presence of 8ml concentration of agave americana extract

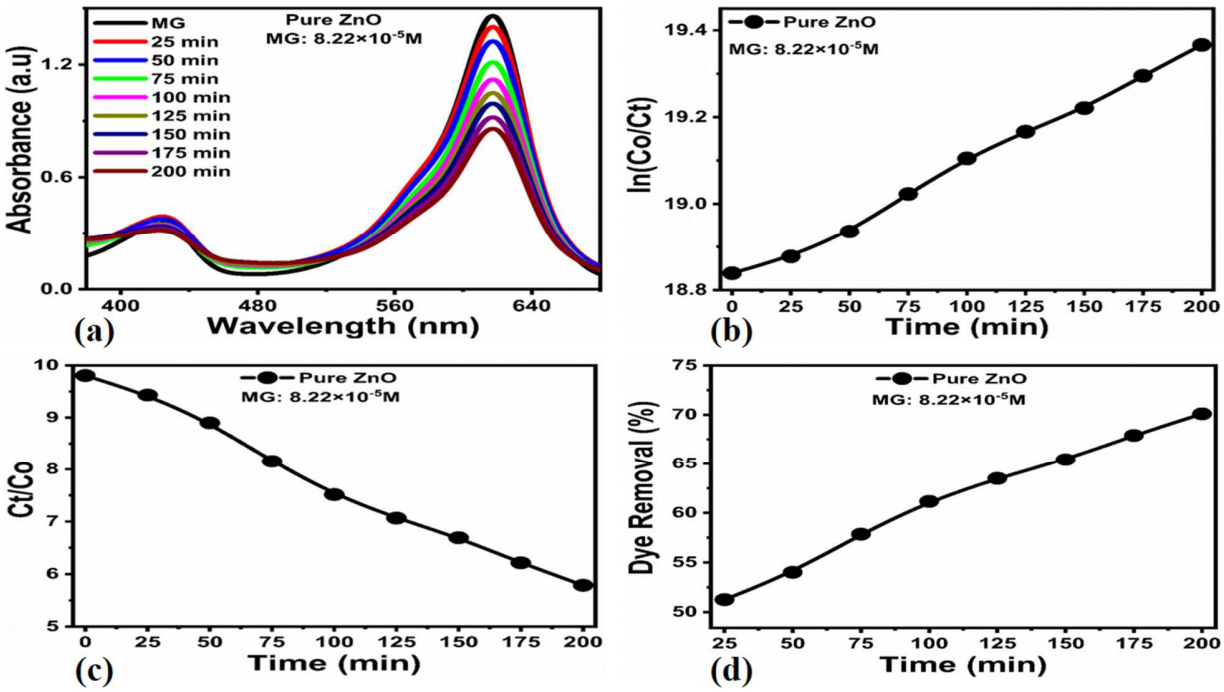

Figure 6. (a) UV-Visible absorption spectra of Pure ZnO **(b)** 1st order pseudo-kinetics process of photodegradation of 8.22×10^{-5}M MG at different time interval **(c)** 2nd order pseudo-kinetics process of photodegradation of MG **(d)** the dye removal percentage of pure ZnO over MG under sun light source from (25-200 min).

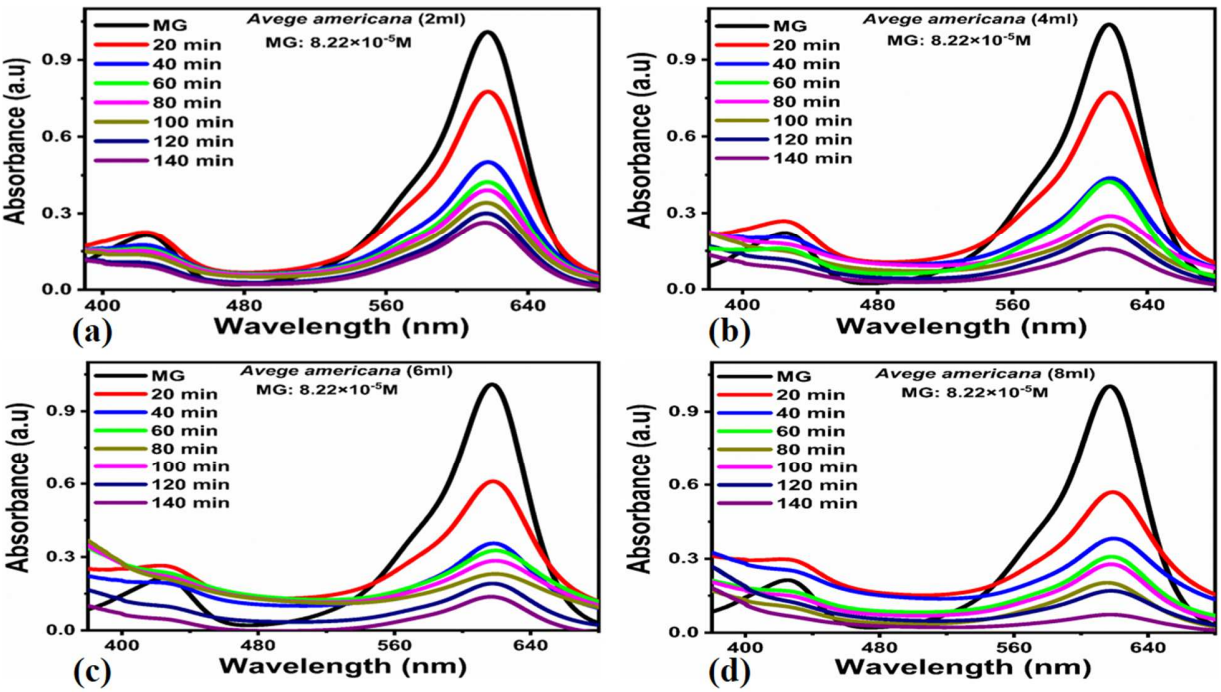

Figure 7. (a-d) UV-Visible absorption spectra of photodegradation for (8.22×10^{-5}M) MG under UV light irradiation over different concentration of ZnO/ agave americana extract (2 mL,4 mL,6 mL and 8 mL) at 20-140 min.

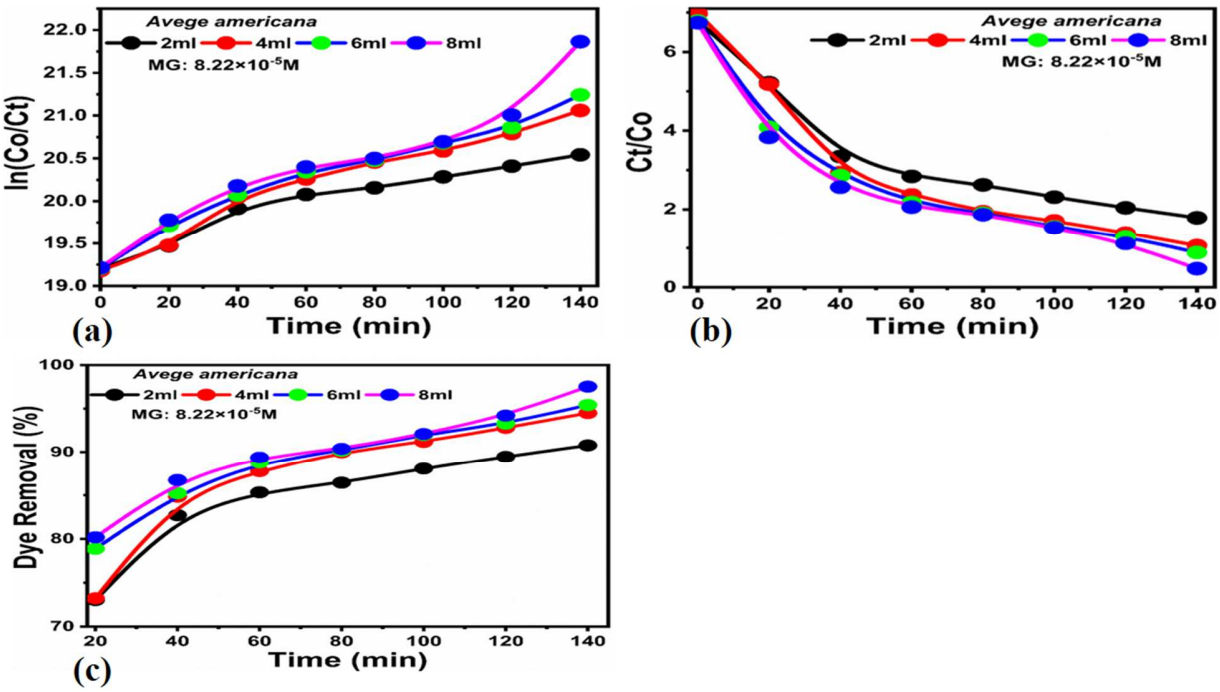

Figure 8. (a-d) UV-Visible absorption spectra of photodegradation for (8.22×10^{-5}M) MG under UV light irradiation over different concentration of ZnO/ agave americana extract (2 mL,4 mL,6 mL and 8 mL) at 20-140 min.

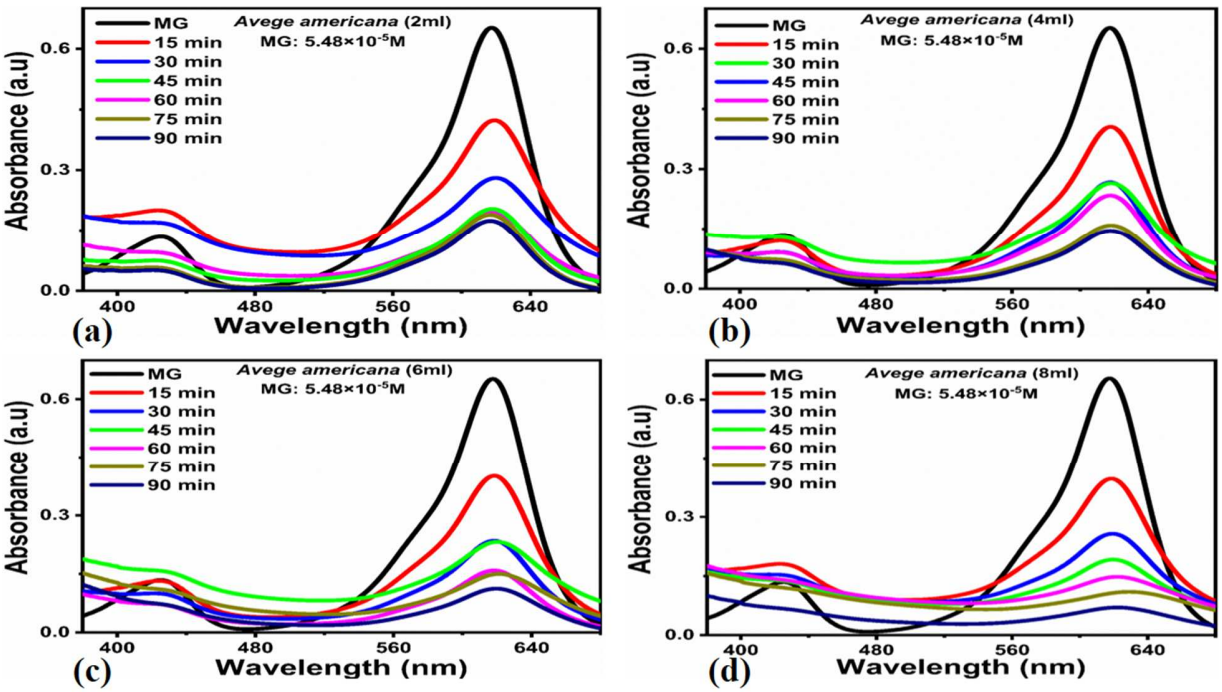

Figure 9. (a-d) UV-Visible absorption spectra of photodegradation for (5.48×10^{-5}M) MG under UV light irradiation over different concentration of ZnO/ agave americana extract (2 mL,4 mL,6 mL and 8 mL) at 20-140 min.

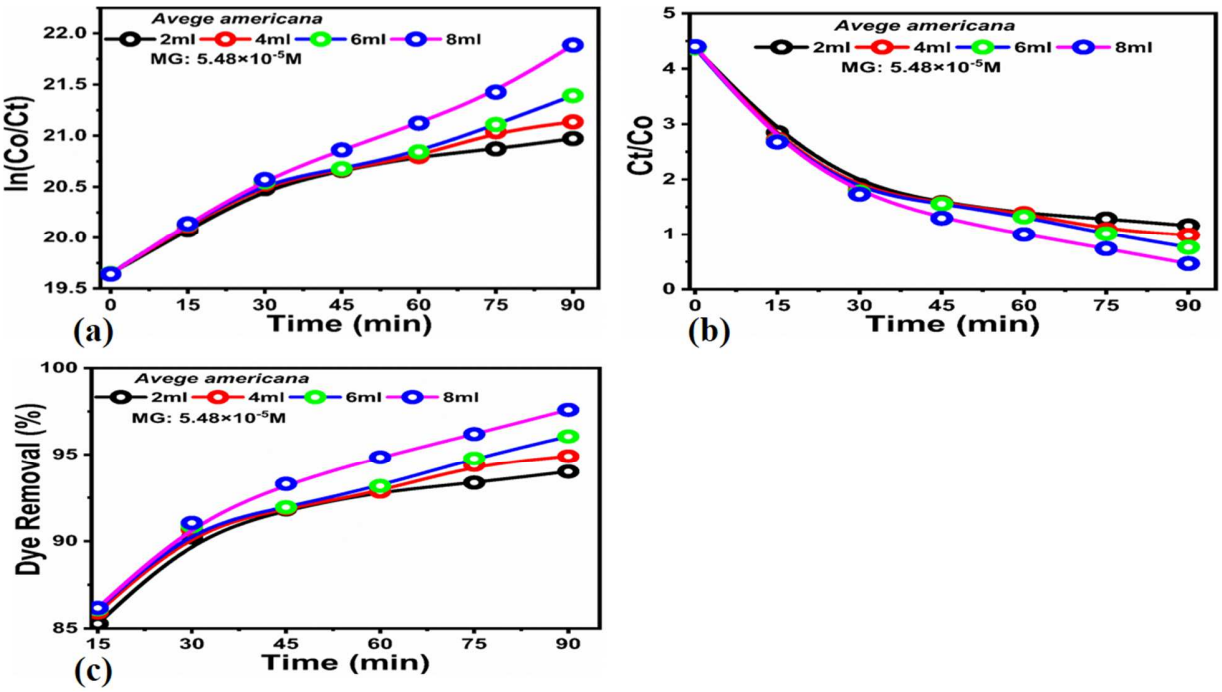

Figure 10. (a-d) UV-Visible absorption spectra of photodegradation for (5.48×10^{-5}M) MG under UV light irradiation over different concentration of ZnO/ agave americana extract (2 mL,4 mL,6 mL and 8 mL) at 15-90 min.

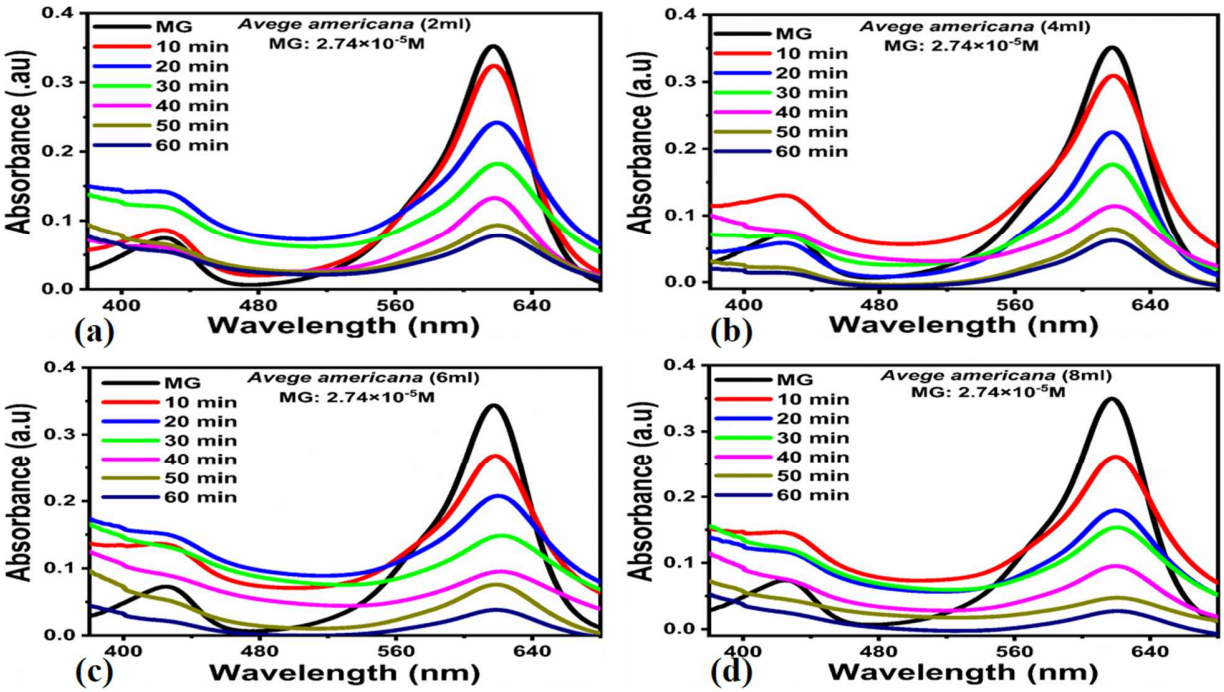

Figure 11. (a-d) UV-Visible absorption spectra of photodegradation for (2.74×10^{-5}M) MG under UV light irradiation over different concentration of ZnO/ agave americana extract (2 mL,4 mL,6 mL and 8 mL) at 20-140 min.

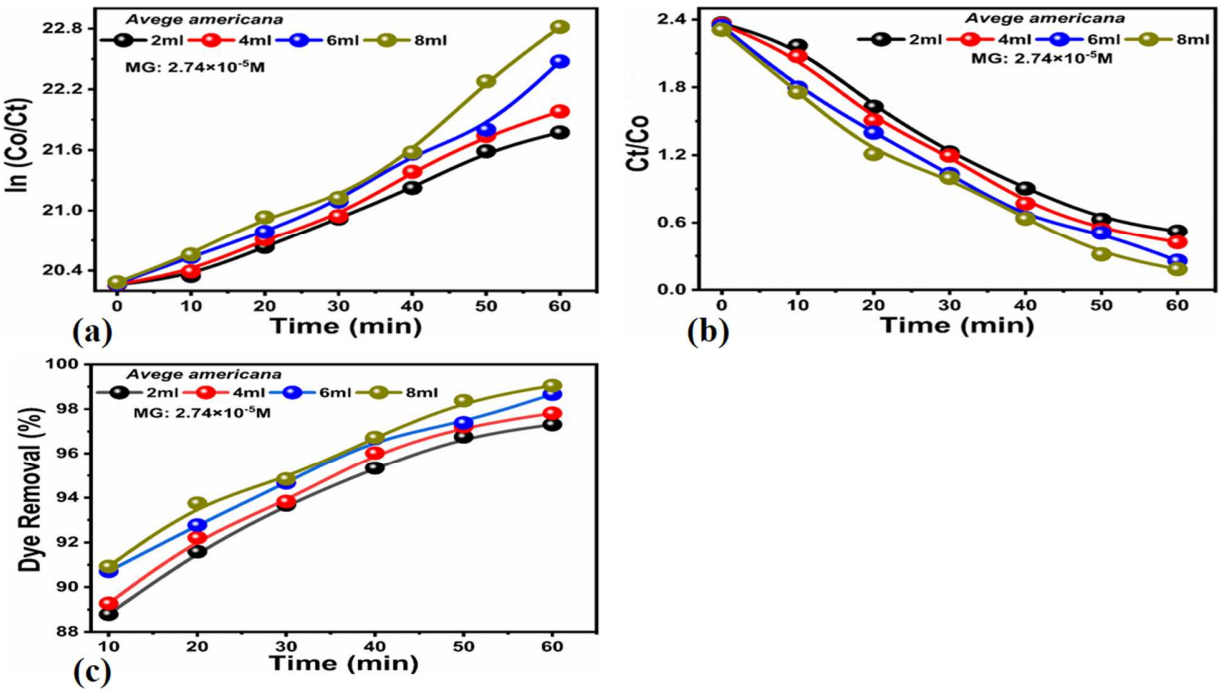

Figure 12. (a-d) UV-Visible absorption spectra of photodegradation for (2.74×10^{-5}M) MG under UV light irradiation over different concentration of ZnO/ agave americana extract (2 mL,4 mL,6 mL and 8 mL) at 10-60 min.

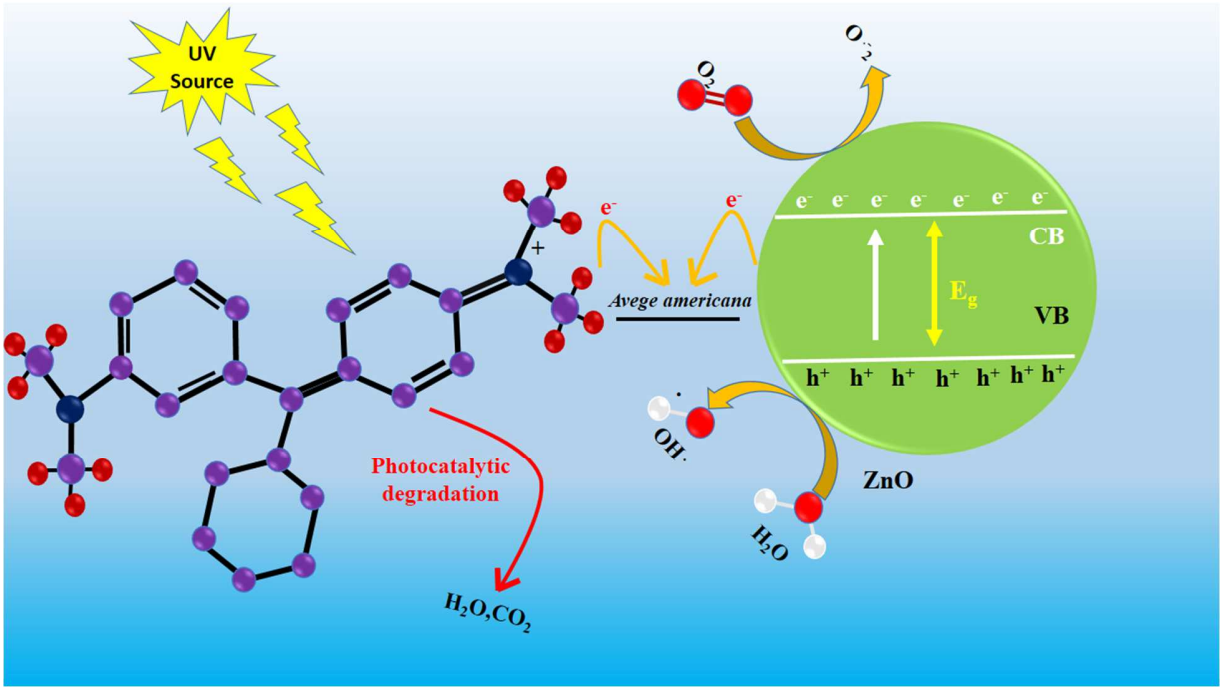

Figure 13. Simple photocatalytic degradation mechanism of the ZnO/ agave americana extract over MG dye in the illumination of UV light irradiation.

Table1: Calculated average crystallite size (nm) for pure ZnO and other ZnO samples prepared in the presence of various amounts of agave americana extract

Name of Samples	**2(θ)**			**Average particle size (nm)**
	100	**002**	**101**	
Pure ZnO	31.3	34.0	35.8	19.6
2ml	31.4	34.3	36.1	19.3
4ml	31.5	34.3	36.4	17.0
6ml	31.7	34.5	36.7	16.3
8ml	32.2	35.2	36.9	14.6

Table 2: Calculated rate constants of various ZnO samples thermally treated with various amounts of agave americana extract

Name of Samples	Dye Conc.	Rate Constant (K)	Dye conc.	Rate Constant (K)	Dye conc.	Rate Constant (K)
Pure ZnO	----------	----------	----------	----------	8.22×10^{-5}M	0.0272 min^{-1}
2 mL	2.74×10^{-5}M	0.2718 min^{-1}	5.48×10^{-5}M	0.1402 min^{-1}	-	0.0907 min^{-1}
4 mL	-	0.3042 min^{-1}	-	0.1566 min^{-1}	-	0.1283 min^{-1}
6 mL	-	0.3546 min^{-1}	-	0.1782 min^{-1}	-	0.1307 min^{-1}
8 ml	-	0.4171 min^{-1}	-	0.235 min^{-1}	-	0.1568 min^{-1}

Table 3: Comparison of photocatalytic activity of synthesized ZnO nanostructures for the degradation of MG with previous reported works

Catalysts	MG Dyes concentration	Time(min)	Removal %	Reference
ST/PL(AA-cl-AAm)/Fe/Zn NCHG	2X10-6 M	300	91	55
ZEDTA	$1 \times 10{-}5$ M	61	94.14	56
CDC	$2.18 \times 10{-}5$ M	90	93	57
(rGO/CuS-7	$3.64 \times 10{-}5$ M	90	97.6	58
ZnO NPs	$3.64 \times 10{-}5$ M	180	99	59
$CeFeO_3$	$2 \times 10{-}5$ M	120	91	60
L-CMTS	$0.72 \times 10{-}5$ M	140	95	61
$CoMn_2O_4$	$1.370 \times 10{-}5$ M	60	87	62
$ZnO/GdCoO_3$	$6.0 \times 10{-}6$ M	120	92.4	63
Biosynthesized ZnO NPs	$4.56 \times 10{-}5$ M	160	91.2	64
$CuFe_2O_4$@BC	5×10^{-5}M	90	98.9	65
CoCA	1×10^{-5} M	100	91.2	66
ZnO/Punica granatum	10ppm	40	99.0	67
ZnO paste	20 mg/ L	16	97.5	68
ZnO / agave americana extract	2.74×10^{-5}M	60	99.0	**Present work**